

Water-Resistant, Transparent Hybrid Nanopaper by Physical Cross-Linking with Chitosan

Matti S. Toivonen,[†] Sauli Kurki-Suonio,[†] Felix H. Schacher,[‡] Sami Hietala,[§] Orlando J. Rojas,^{||} and Olli Ikkala*,[†]

[†]Molecular Materials, Department of Applied Physics, Aalto University (previously Helsinki University of Technology), P.O. Box 15100, FIN-00076 Aalto, Espoo, Finland

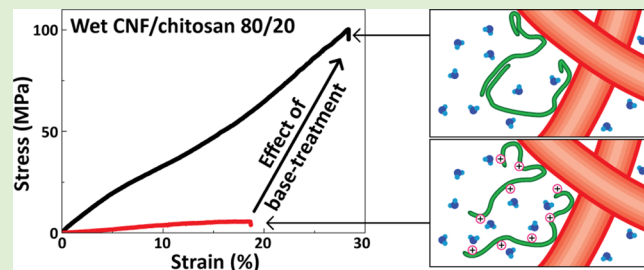
[‡]Institut für Organische Chemie und Makromolekulare Chemie und Jena Center for Soft Matter, Friedrich-Schiller-Universität Jena, Lessingstraße 8, 07743 Jena, Germany

[§]Laboratory of Polymer Chemistry, Department of Chemistry, University of Helsinki, P.O. Box 55, FIN-00014 HY, Helsinki, Finland

^{||}Bio-Based Colloids and Materials, Department of Forest Products Technology, Aalto University, P.O. Box 16300, FIN-00076 Aalto, Espoo, Finland

Supporting Information

ABSTRACT: One of the major, but often overlooked, challenges toward high end applications of nanocelluloses is to maintain their high mechanical properties under hydrated or even fully wet conditions. As such, permanent covalent cross-linking or surface hydrophobization are viable approaches, however, the former may hamper processability and the latter may have adverse effect on interfibrillar bonding and resulting material strength. Here we show a concept based on physical cross-linking of cellulose nanofibers (CNF, also denoted as microfibrillated cellulose, MFC, and, nanofibrillated cellulose, NFC) with chitosan for the aqueous preparation of films showing high mechanical strength in the wet state. Also, transparency (~70–90% in the range 400–800 nm) is achieved by suppressing aggregation and carefully controlling the mixing conditions: Chitosan dissolves in aqueous medium at low pH and under these conditions the CNF/chitosan mixtures form easily processable hydrogels. A simple change in the environmental conditions (i.e., an increase of pH) reduces hydration of chitosan promoting multivalent physical interactions between CNF and chitosan over those with water, resulting effectively in cross-linking. Wet water-soaked films of CNF/chitosan 80/20 w/w show excellent mechanical properties, with an ultimate wet strength of 100 MPa (with corresponding maximum strain of 28%) and a tensile modulus of 4 and 14 GPa at low (0.5%) and large (16%) strains, respectively. More dry films of similar composition display strength of 200 MPa with maximum strain of 8% at 50% air relative humidity. We expect that the proposed, simple concept opens new pathways toward CNF-based material utilization in wet or humid conditions, which has still remained a challenge.



INTRODUCTION

Cellulose nanofibers (CNF) are nanoscale fibrillar materials (schematic representation in Figure 1a) that have drawn significant attention in recent years due to their excellent mechanical properties based on their native hydrogen bonded internal crystalline structure, renewability, availability, and biocompatibility.^{1,2} It allows mechanically strong compositions, leading to several potential applications, including structural materials, gas barriers in packaging, templates for functional materials, and substrates for transparent electronics and devices.^{3–11} The strength of the junctions between CNF forming the disordered networks is central to transfer the high mechanical properties of the individual nanofibers up to the macroscopic material. Such interactions can be subtle, involving hydrogen bonding and other interactions. Upon hydration by elevated ambient humidity or direct contact with water, the junctions between the CNF weaken and the resulting material

suffers from loss of mechanical properties since water molecules penetrate into the network and compete with the interfibrillar bonds.^{12,13} This can become a serious issue in applications, as CNF is inherently highly hygroscopic. The mechanical properties in the wet state can be improved by covalent cross-linking, either directly between the cellulose nanofibers or mediated by cross-linkable polymer matrices. In the first case, simply heating can lead to the formation of ester bonds between carboxyl and hydroxyl groups in cellulose, as first reported for papermaking fibers, an effect that can be augmented in the presence of polyacids to yield a high wet strength.^{14,15} Such observations can be translated to nanocellulose, as demonstrated more recently.¹⁶ In the second case

Received: February 2, 2015

Revised: February 9, 2015

Published: February 9, 2015

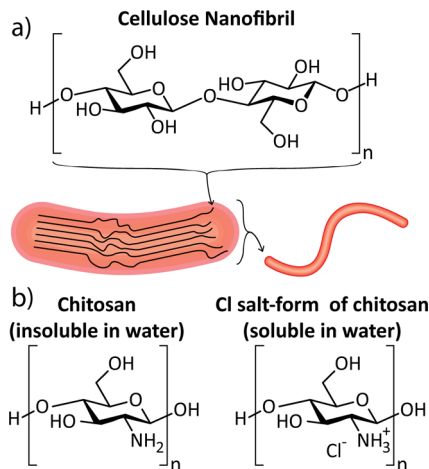


Figure 1. (a) Molecular structure of cellulose and illustration of cellulose chains forming cellulose nanofibrils (CNF) with the crystalline and amorphous domains. The surface-bound residual heteropolysaccharides are not shown. (b) Molecular structure of chitosan in the neutral and charged forms.

of cross-linkable polymer matrices, reported efforts with MFC/CNF have included phenolic resins, melamine formaldehyde, and epoxy, among others.^{17–19} However, covalent cross-links bind the structures permanently and therefore hamper post-and reprocessing. Covalent cross-linking can also lead to loss of toughness as is commonly seen in rigid and brittle covalently cross-linked hydrogels and thermoset polymers.^{20,21} Also, most of the methods demand multiple steps, which limits scalability.

An alternative to covalent cross-linking of CNF-based materials is to incorporate physical cross-linking, which has been recognized as a viable pathway to tough hydrogels, thus, enabling retention of attractive mechanical properties even in the wet state.^{22–24} Individual physical cross-links are typically weaker than covalent ones, making them more likely to break and possibly rearrange upon stress, potentially serving as sacrificial bonds for dissipating energy during deformation.²⁵ Polysaccharides and, more generally, carbohydrate-containing polymers provide a class of materials that bind onto cellulose surfaces by multivalent physical interactions and can function as physical cross-linkers for CNF.^{26–29} Physical cross-links could also be tunable according to environmental parameters, such as temperature or pH, and could offer the benefit of inducing cross-links that are reversible, allowing processing, as recently shown for thermoreversible cellulose nanocrystal/methyl cellulose hydrogels.³⁰ Physical cross-linking could potentially be of practical importance also in fiber spinning of CNF.^{31–33} Therein, silk may provide inspiration for new approaches, as there the transition from the fluid starting dope into the final fibrous state occurs by environmental stimuli.³⁴ Concepts inspired by this could allow CNF processing in the wet state followed by subsequent physical structural interlocking.

Here we report a simple route for preparing a hybrid nanopaper with good mechanical properties under wet water-soaked conditions due to physical cross-linking. First, CNF is mixed with chitosan to form visually homogeneous, viscous aqueous mixtures that are solvent cast and, importantly, subsequently treated with a base to insolubilize chitosan within the CNF network to interlock the structures. In addition, we report that the films are highly transparent. Creating such a wet-strong and transparent hybrid nanopaper of CNF and a polysaccharide requires that conditions are identified where the

components can be homogeneously mixed while preventing aggregation.^{35,36} A stimulus-responsive polymer, which can transition from water-soluble to insoluble, can have the benefit of not cross-linking the system in the soluble, processable state during mixing and cross-linking upon the appropriate stimulus. Chitosan is a pH-responsive polysaccharide that readily adsorbs on cellulose surfaces, which is relevant for the resulting wet strength.^{37–39}

Chitosan is a biocompatible polysaccharide produced by deacetylation from chitin, an abundant biopolymer mainly extracted from the exoskeleton of crustaceans.⁴⁰ Chitosan has drawn significant attention due to its attractive mechanical properties, sustainability, biocompatibility, and antimicrobial properties.^{41–43} Additionally, chitosan has shown potential as a wet strength agent for paper, highlighting its capability to bind cellulosic fibers.^{44–47} The backbone of chitosan consists of N-acetylglucosamine and D-glucosamine units of which the latter contain primary amines that make the polymer pH-responsive. Chitosan is water-soluble when the amines are ionized (see Figure 1b), roughly below the pK_a of the ammonium ion, between 6.0 and 6.5.^{48,49}

Here we report CNF/chitosan mixtures encompassing a wide composition range and a route to allow wet-strong films upon base-treatments. We describe mechanical properties in the fully wet state, also showing results under more dry state as a reference, as well as show high transparency and alignment resulting from stretching.

EXPERIMENTAL SECTION

Materials. CNF was prepared from never dried birch pulp by disintegrating the pulp 20 times through a fluidizer (Microfluidics Corp., Newton, MA, U.S.A.), leaving a hydrogel with a consistency of approximately 2.11 wt %. Chitosan from crab shells delivered as dry flakes of middle viscosity ($M_w = 300–500$ kDa, degree of deacetylation = 80% determined by acid–base titration, see text below) and high viscosity ($M_w = 500–700$ kDa, degree of deacetylation = 75% determined by acid–base titration, see text below), 37% hydrochloric acid, sodium hydroxide and sodium sulfate were purchased from Sigma-Aldrich. Ammonium hydroxide (28–30%), acetic acid (>99.8%), and tris(hydroxymethyl)aminomethane were acquired from Sigma-Aldrich. Ammonium formate and formic acid (98–100%) were acquired from Riedel-de Haën. Arabinose (99.8%) was purchased from Calbiochem. Rhamnose and glucose (>99%) were purchased from BDH Prolabo. Galactose (>98%), xylose (>99%), and mannose (>98.0%) were purchased from Merck. Deionized water was obtained with a Milli-Q water system from Millipore.

Preparation of the Buffer Solutions. Buffer solutions were prepared by combining ammonium hydroxide with formic acid for buffers of pH 4.0 and 9.1 and tris(hydroxymethyl)aminomethane with acetic acid for buffers of pH 5.7 and 6.8. Ammonium formate was dissolved in deionized water at 1 M. Ammonium hydroxide and formic acid were diluted to 1 M with deionized water. Ammonium hydroxide (1 M) or formic acid (1 M) was added to 1 M ammonium formate until the pH reached the desired value. Acetic acid was diluted to 1 and 2 M stock solutions. Tris(hydroxymethyl)aminomethane was dissolved in a 2 M stock solution with deionized water. Acetic acid (2 M) and tris(hydroxymethyl)aminomethane (2 M) were combined in a 1:1 ratio to give 1 M tris-acetate. For pH 5.7 tris-acetate buffer, 1 M acetic acid was added to 1 M tris-acetate until pH reached the desired value. Tris-acetate solution (1 M) was used without further addition of acid or base for pH 6.8 tris-acetate buffer. Before use, the 1 M buffer solutions were diluted to 100 mM with deionized water. Buffer solutions (100 mM) with divalent anion for ionic cross-linking of chitosan were prepared by dissolving sodium sulfate in 100 mM buffer solutions to give 100 mM sodium sulfate. pH was measured with an electronic pH meter (6230N, JENCO).

Preparation of Mixtures of CNF and Chitosan and Film Casting. Chitosan was dissolved at 0.2 wt % in 12 mM HCl, which had been diluted with deionized water. Dissolution time was 24 h at minimum. After dissolution, the solution was filtered with a syringe filter (Acrodisc 25 mm Syringe Filter w/5 μm Versapor Membrane, PALL). The CNF gel was diluted to 0.3 wt % by adding deionized water followed by vigorous stirring for 24 h. The diluted CNF dispersion was then centrifuged at 5000g for 60 min to remove aggregates. The sediment was discarded and the supernatant was used for sample preparation. The carbohydrate compositions and the molar masses of the original CNF dispersion, the sediment, and the supernatant were determined as described below. It was observed that the weight-averaged molar mass was lower in the supernatant and hemicellulose content was higher. Values are listed in Table S1. The mass concentration of CNF in the obtained supernatant was determined by weighing a given amount of the dispersion and drying it overnight in an oven at 50 °C followed by weighing. The final dry mass divided by the initial mass of the dispersion to yield the reported mass percentage of the dispersion. The values obtained were in the range of 0.17 to 0.19 wt %. The used supernatant will be referred to as CNF in the rest of the text.

CNF was dispersed in deionized water prior to mixing with 0.2 wt % chitosan in 12 mM HCl. Dissolved chitosan and CNF were combined by measuring a given amount of 0.2 wt % chitosan solution in a glass bottle. CNF dispersion was added until a desired dry mass ratio between chitosan and CNF was reached. The mixtures will hereafter be called CNF/chitosan [dry wt % of CNF]/[dry wt % of chitosan]. The acid concentration of the mixture depended on the mixing ratio, as the CNF dispersion contained no acid. The total dry mass was approximately 120 mg, and the volumes were in the range of 50–80 mL. The mixture was homogenized with a high-shear homogenizer (Ultra Turrax T25 basic IKA Labortechnik) for 10 min at 11000 rpm/min. Films were cast on polystyrene Petri dishes (diameter 86 mm) followed by evaporation under ambient conditions in a fume hood on a horizontal surface. The dried films were cut in two halves of which one was immersed in 100 mM aqueous NaOH solution for 15 min followed by repeated rinsing with deionized water until pH of rinsing water was 7. This half will be hereafter referred to as “base-treated”. The other half was used as a reference sample and treated for 15 min with deionized water. This half will be hereafter referred to as “not base-treated”. After draining excess water out, the films were left to dry by evaporation in ambient conditions.

Tensile Properties. The films were cut into strips 2.25 mm wide and more than 1.5 cm long by pressing with a custom-made razor blade jig, where multiple flat blades are evenly spaced by flat metal spacers and tightened parallel to each other. For clamping, the strips were glued from both ends onto small pads of abrasive paper (ca. 3 mm × 4 mm), leaving a 10 mm long strip available for standard tensile tests. The widths of the strips were measured with an optical microscope (Leica MZ6 equipped with a Leica DFC420 camera). The thicknesses of the films were measured with a film thickness measurement setup composed of a displacement sensor (LGF-0110L-B, Mitutoyo), digital reader (EH-10P, Mitutoyo), and a measuring table with support for sensor (215–514 comparator stand, Mitutoyo). For mechanical characterization in the wet state samples were either first clamped to the tensile tester (Tensile/Compression Module 5 kN with 100 N load cell, Kammerath & Weiss GmbH) and soaked for 60 s with deionized water or soaked for 48 h in a buffer solution before measurement. A total of 60 s was found to be sufficient for equilibration based on mechanical behavior (see Figure S4). One set of base-treated CNF/chitosan 80/20 samples were soaked for 60 s with 100 mM HCl instead of deionized water. Dry samples were equilibrated in a custom-made humidity chamber inside which also the tensile tester was located. Rate of elongation was 0.5 mm/min and gauge length was 10 mm. Optical video between crossed polarizers was recorded for most of the soaked samples. For this, the sample was illuminated from below through a polarizing film with the polarization direction at 45° angle with the sample elongation direction. Another polarizer was attached at the camera lens with 90° angle with the first polarizer.

Scanning Electron Microscopy (SEM). Dry films of the supernatant and the sediment of CNF after centrifugation were prepared by pipetting a small amount onto a silicon wafer attached to aluminum SEM stubs with carbon tape. An approximately 15 nm thick gold film was sputtered (Emitech K100X). Imaging was carried out with a Zeiss Sigma VP scanning electron microscope at 1–2 kV acceleration voltage.

Transmission Electron Microscopy (TEM). Micrographs were imaged in bright field mode with a Tecnai 12 Bio Twin instrument (FEI), operating at an accelerating voltage of 120 kV, and recorded with an Ultra-Scan 1000 CCD camera (Gatan). CNF/chitosan 80/20 w/w mixtures prepared from 0.18 wt % CNF and 0.2 wt % chitosan in 12 mM HCl were diluted to approximately 0.01 wt % with deionized water. A total of 3 μL of the diluted mixture was pipetted onto a copper TEM grid with a holey carbon film and allowed to stand for 60 s before draining the excess by blotting. Chitosan in the sample was subsequently stained with methyl iodide vapor for 10 min in a closed vial to enhance contrast.

Rheology. TA AR2000 stress-controlled rheometer equipped with an aluminum double gap cylinder was used for rheological characterization. Oscillatory frequency sweeps were made in the linear viscoelastic range (2%) at 20 °C verified by strain sweeps. The flow properties were measured from low to high shear rates. All measurements on CNF/chitosan mixtures were carried out on freshly prepared samples.

Determination of Carbohydrate Composition of CNF. The carbohydrate compositions of the original CNF prior to centrifugation, the supernatant, and the sediment were determined as previously reported.⁵⁰ Briefly, dried sample (0.3 g) was weighed in a predried crucible. A total of 3 mL of 72% sulfuric acid was added with stirring. The sample was hydrolyzed for 60 min with stirring in a 30 °C water bath. After hydrolysis, the acid was diluted to 4% concentration by adding 84 mL deionized water, the crucible was sealed and autoclaved for 1 h at 121 °C. After cooling to room temperature, the hydrolysis liquor was filtered through a 0.2 μm syringe filter. Double injections of the samples were analyzed with High-Pressure Anion Exchange Chromatography (HPAEC, Dionex ICS-3000 Ion Chromatography System) against calibration standards of arabinose, rhamnose, galactose, glucose, xylose, and mannose with concentrations 1, 10, 25, and 50 mg/L.

Determination of Molecular Weight-Average Masses of Polysaccharides in CNF. The molar masses of the polymeric components of CNF were determined by analytical size exclusion chromatography (SEC). Approximately 50 mg of dry sample was dispersed in 5 mL of water from where they were solvent-exchanged first to acetone. Acetone was exchanged further to *N,N*-dimethylacetamide (DMAc) and finally to 90 g/L LiCl in DMAc solution (90 g/L LiCl/DMAc), where the samples were dissolved. The solution was diluted with pure DMAc to give approximately 1 g/L of sample in 9 g/L LiCl/DMAc solution and filtered with 0.2 μm syringe filters. The SEC-analysis was performed with a Dionex Ultimate 3000 chromatography system that comprised one guard column (PLgel Mixed-A, 7.5 × 50 mm, Agilent Technologies) and four analytical columns (PLgel Mixed-A, 7.5 × 300 mm) in series and an RI-detector (Shodex RI-101). The 9 g/L LiCl/DMAc solution was used as the eluent, with a flow rate of 0.75 mL/min. The analysis was carried out at room temperature. Double injections of 100 μL were conducted for each sample. Narrow pullulan standards (343 Da–708 kDa, from Polymer Standard Service GmbH, and 1600 kDa from, Fluka GmbH) were used for calibration. The molar mass distributions were calculated with a custom-made MATLAB script.

Determination of Degree of Deacetylation. The degree of acetylation of the chitosan samples was determined as previously reported.⁵¹ Briefly, dried chitosan (0.2 g) was dissolved in 20 mL of 100 mM HCl (aq) and 25 mL of water. After 30 min continuous stirring, deionized water (25 mL) was added and stirring for 30 min. Upon complete dissolution of chitosan, the solution was titrated with a 0.1 mM NaOH (aq) solution and the degree of deacetylation (DA) according to eq 1:

$$\text{DA}\% = 2.03 \frac{V_2 - V_1}{m + 0.0042(V_2 - V_1)} \quad (1)$$

where m is weight of sample in grams and V_1 and V_2 are the volumes of 0.1 mM NaOH (aq) solution corresponding to the deflection points in milliliters; 2.03 is a constant resulting from the molecular weight of chitin monomer unit and 0.0042 is a coefficient resulting from the difference between molecular weights of chitin and chitosan monomer units.

Ultraviolet–Visible Light (UV–vis) Spectroscopy. Transmission spectra of thin films (approximately 12 μm thick) were recorded in UV–visible range with PerkinElmer Lambda 950 UV/vis/NIR absorption spectrophotometer.

Wide-Angle X-ray Scattering (WAXS). WAXS measurements were performed on a Bruker AXS NanoStar-U Instrument equipped with a microfocus X-ray source (Incoatec I μ S Cu E025) operating at $\lambda = 1.54 \text{ \AA}$. A pinhole setup with pinhole diameters 750, 400, and 1000 μm (in order from source to sample) was used and the sample-to-detector distance was 4.95 cm (calibrated with silver behenate). The beam was incident perpendicular to the plane of the films. Intensity distribution profiles in the azimuthal angle for 2θ values ranging from 18 to 24° (intensity maximum at 21°) wherein lies the (200) reflection, were used to calculate the Hermans orientation parameter (S) according to the eqs 2 and 3:^{52,53}

$$S = \frac{3}{2} \langle \cos^2 \Phi \rangle - \frac{1}{2} \quad (2)$$

with

$$\langle \cos^2 \Phi \rangle = \frac{\sum_0^\pi I(\Phi) \sin \Phi \cos^2 \Phi}{\sum_0^\pi I(\Phi) \sin \Phi} \quad (3)$$

Samples from base-treated CNF/chitosan 80/20 w/w films were prepared for WAXS similarly as those for tensile characterization. After clamping and soaking with deionized water, the films were stretched to a predetermined strain and excess water was drained by carefully touching with the corner of a tissue. Subsequently, the load was allowed to stabilize prior to relaxation of the film in order to prevent shortening from shrinking. Finally, the samples were relaxed and allowed to fully dry. Used strains were 5, 10, 15, and 20%. The unstrained samples were taken directly after base-treatment without further processing. Strains higher than 20% led to rupture of the films during drying in tension. Some shrinking during drying was observed in the form of slight curling of the films.

RESULTS AND DISCUSSION

A homogeneous aqueous mixture of CNF and chitosan is possible when chitosan remains soluble and CNF does not flocculate or aggregate. Electrostatic stabilization of CNF is reduced at low pH as carboxylic acids within the surface-bound residual heteropolysaccharides lose charge and CNF flocculates due to the suppression of the electrostatic colloidal stabilization. This can be seen by adding a small amount of acid to a CNF dispersion (see Figure S1). Chitosan is soluble only in an acidic solution and aggregates from solution if pH is increased above its pK_a , which is between 6.0 and 6.5, to deionize the primary amines of the chitosan backbone.^{48,49} Therefore, a homogeneous mixture of these components can only be achieved within a narrow pH window. This is somewhat complicated by the buffering capability of both the amines in the chitosan and the carboxylic acids in CNF combined with the possibility of stabilization of CNF by adsorbed chitosan.

Visually homogeneous mixtures were achieved when mixing 0.2 wt % chitosan dissolved in aqueous 12 mM HCl with 0.17–0.2 wt % CNF dispersed in deionized water which resulted in a pH of 3.4 in the final mixture. When 0.2 wt % chitosan in 8 mM or 16 mM HCl (aq) were used, correspondingly, the mixtures

turned out inhomogeneous (see Figure S2). The suggested behaviors of the CNF/chitosan mixtures in solutions of low, medium, and high pH (pH 2.8, 3.4, and 4.5, respectively) are shown in Figure 2. Low pH (mixture pH 2.8, using 0.2 wt %

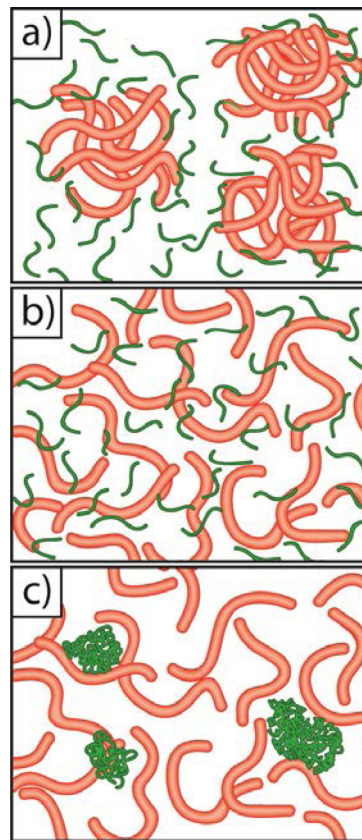


Figure 2. Schematic representation (not to scale) of the colloidal behavior upon mixing of CNF/chitosan in (a) low pH where CNF flocculates due to the surface-bound heteropolysaccharides, (b) optimal pH where both components remain stable and, (c) high pH where chitosan aggregates.

chitosan in aq 16 mM HCl) drives flocculation of CNF in solution. High pH (mixture pH 4.5, using 0.2 wt % chitosan in aq 8 mM HCl) causes aggregation as chitosan cross-links CNF prior to mixing. When pH is suitable (mixture pH 3.4, using 0.2 wt % chitosan in aq 12 mM HCl), chitosan remains dissolved and flocculation of CNF is negligible. Chitosan adsorbed on CNF may provide further stabilization even at pH lower than what would make CNF alone to flocculate.

Visually homogeneous and translucent CNF/chitosan aqueous mixtures were obtained using the procedure shown in Figure 3. The interactions of CNF and chitosan upon mixing at 80/20 w/w ratio resulted in a slight increase in viscosity and turbidity and the mixture displayed a visible elastic response to agitation. This was confirmed by rheology by inspecting the storage (G') and loss (G'') moduli as a function of the angular frequency ω , see Figure 4a. For CNF/chitosan 80/20 w/w mixtures, $G' \sim \omega^0$ and $G' \gg G''$, indicating gelation. Also, pure CNF showed enhanced elasticity at the present low concentration, but the moduli were considerably lower. Pure chitosan was a very low viscosity fluid, with moduli that were in the lower limit of detection of the measuring unit, and are therefore not included in Figure 4a. At low shear rates, the CNF/chitosan 80/20 w/w mixture showed much higher

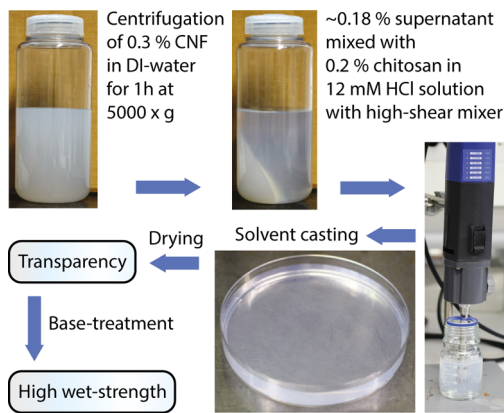


Figure 3. Method to prepare the CNF/chitosan mixtures and casting of transparent hybrid nanopaper with good mechanical properties in both the wet and dry states.

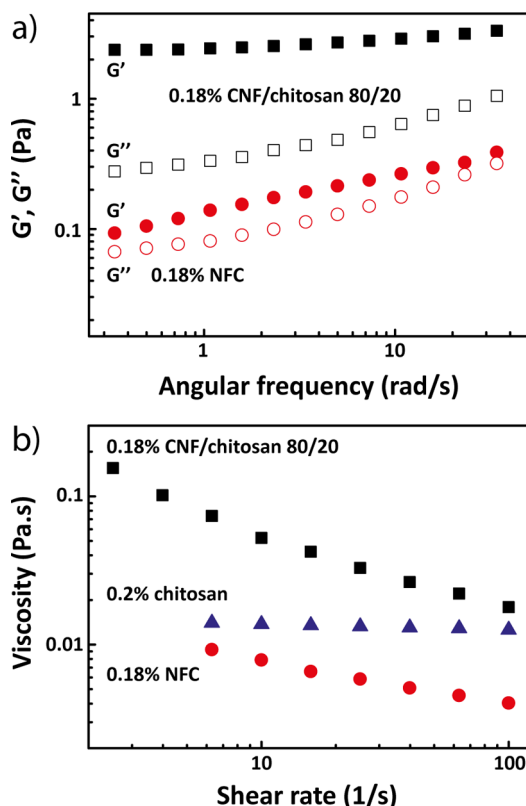


Figure 4. (a) Rheological moduli and (b) viscosities of CNF 0.18 wt % supernatant in deionized water (black squares), 0.2 wt % chitosan in 12 mM HCl (blue triangles), and mixture of CNF/chitosan 80/20 w/w (red circles). At these low concentrations, pure chitosan flows as a liquid at low shear rates, and the respective moduli data are not presented in the figure, as they cannot be reliably measured.

viscosity (see Figure 4b) than the pure components indicating strong CNF–chitosan interactions. The CNF and the mixture were both shear thinning, which has also been observed earlier for pure CNF dispersions.⁵⁴ Finally, we point out that the high viscosity values shown in Figure 4b suggests the use of low concentrations to prepare the mixtures, in order to obtain homogeneous mixtures even at very high CNF-to-chitosan ratios.⁵⁵

Mechanical Properties. For the mechanical characterization, the films were cut in half and one part was immersed in

100 mM NaOH (aq) solution and the other part in deionized water for 15 min followed by thorough rinsing with deionized water and drying in ambient conditions by evaporation. The first set of samples are referred to as “base-treated” whereas the latter ones as “not base-treated” (Table S2). The dry films were cut and prepared for the tensile characterization. After clamping the samples to the tensile tester they were fully soaked by pipetting deionized water on the samples and waiting 60 s before testing. This soaking time was found to be sufficient, as results were similar to base-treated samples soaked in deionized water for even 48 and 72 h (Figure S4). The not base-treated CNF/chitosan 50/50 and 25/75 w/w films are excluded from the data set due to excessive shrinkage and wrinkling, which prevented reliable mechanical testing.

Treatment with 100 mM NaOH solution has a drastic positive effect on the wet tensile properties of all films at all mixing ratios, see Table S2. This effect is illustrated for CNF/chitosan 80/20 showing high wet tensile strength of nearly 90 MPa for the base-treated sample, which indicates a 15-fold increase in comparison to that of the not base-treated equivalent, see Figure 5b. Already the very low chitosan

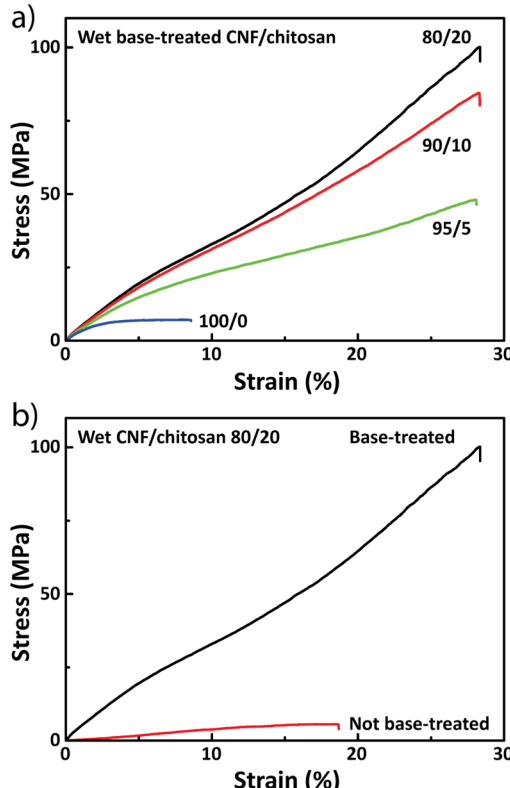


Figure 5. (a) Effect of mixing ratio on wet tensile properties of base-treated CNF/chitosan. (b) Wet tensile properties for base-treated and not base-treated CNF/chitosan 80/20 w/w, illustrating the large effect of the base treatment.

content of CNF/chitosan 95/5 w/w leads to a 3-fold increase in the tensile strength under wet conditions and nearly a doubling of the maximum strain. The tensile strengths and maximum strains in the wet state are significantly higher (e.g., roughly 9-fold higher tensile strength and 3-fold higher maximum strain for CNF/polymer 90/10 w/w composition) in the present work in comparison to those reached with covalent cross-linking of CNF by esterification with poly(acrylic

acid).¹⁶ The increasing tensile strength with chitosan loading is demonstrated in Figure 5a where the stress-strain curves are shown in the wet state for different CNF/chitosan compositions after the base-treatment.

Effect of pH on the Mechanical Properties and Ionic Cross-Linking. To investigate which interfaces are most affected by pH, a CNF/chitosan 80/20 w/w film was characterized under tensile loading after soaking in 100 mM buffer solutions of different pH (9.1, 6.8, 5.7 or 4.0) for 48 h. The results are shown in Figure 6a. The films become

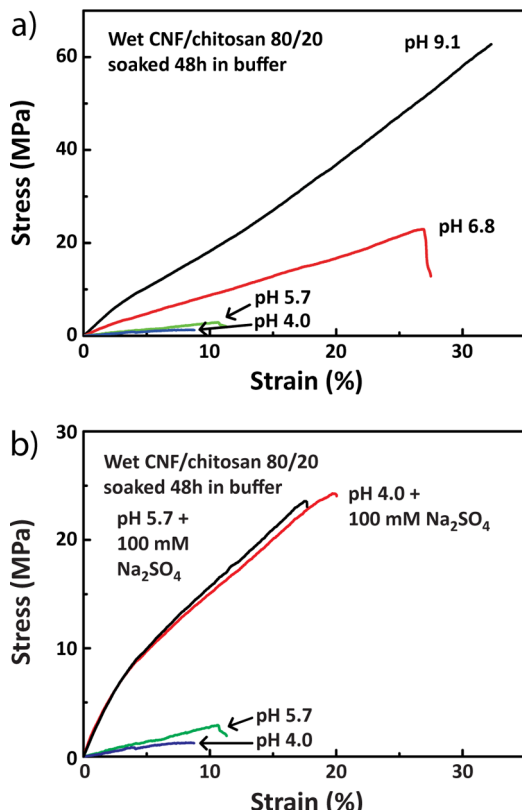


Figure 6. (a) Influence of pH on wet tensile properties of CNF/chitosan 80/20 w/w composites. (b) Ionic cross-linking of chitosan at low pH in the presence of divalent sulfate anions. Samples are soaked 48 h in 100 mM buffer before measurement.

significantly stronger when pH exceeds the pK_a of the ammonium ion in chitosan, which is between 6.0 and 6.5.^{48,49} At low pH (4.0 and 5.7), chitosan is highly charged and bonding between polymer chains is disrupted by electrostatic repulsion and an increased solvation shell around the chains. When a divalent sulfate anion is introduced into the buffer system, it is capable of ionically cross-linking the chitosan chains. This is seen as increases in the wet strength from below 5 to roughly 25 MPa and the wet strain from 10 to 18%, see Figure 6b. If chitosan were to desorb upon dissolution at low pH from the CNF surface, the addition of an ionic cross-linker should not have such a drastic effect on the wet tensile properties. Thus, it is likely that at low pH only the interfaces between chitosan segments are weakened, while chitosan remains strongly adsorbed onto CNF.

Mechanism of Cross-Linking. The proposed mechanism of physical cross-linking of CNF by chitosan is qualitatively illustrated in Figure 7. Three interfaces for bonding are possible and listed in the expected order of increasing strength in the

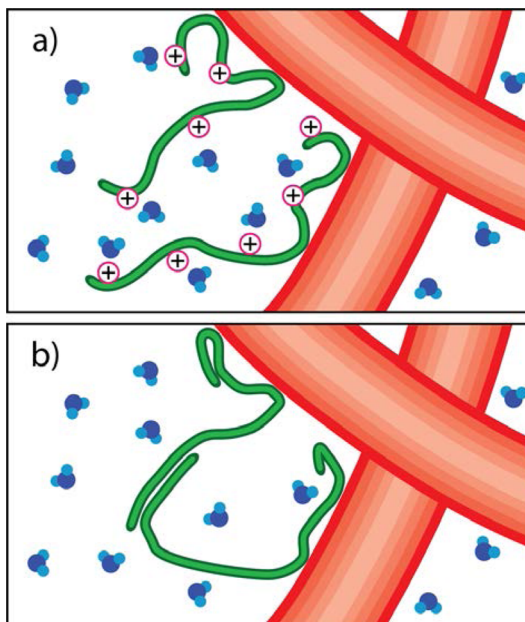


Figure 7. Proposed mechanism of cross-linking of CNF network (thick red fibers) network via chitosan chains (narrow green fibers) in the wet state. (a) Chitosan is charged at low pH leading to electrostatic repulsion and larger hydration layers between chitosan segments in comparison to the case of neutral chitosan at high pH shown in (b).

wet state: those between two fibrils, between chitosan segments, and between fibril and chitosan.

In the dry state, the random CNF network in a film without chitosan is held together mostly by physical interactions between the fibril surfaces. In the presence of water, this interface is severely weakened as these physical bonds compete with water interactions leading to reduced direct interfibrillar hydrogen bonding.¹² It is known that water forms strong hydrogen bonds with polar carbohydrates.^{56,57} This can be interpreted to result in a tight solvation shell effectively blocking interfibril bonding. Overall, the combined effects manifest in a loss of macroscopic mechanical properties under wet conditions as the network is only poorly connected.

Addition of chitosan leads to cross-linking in two steps, starting with the adsorption of chitosan on the CNF surface followed by increased adhesion of dangling segments of chitosan onto available CNF surfaces and other chitosan segments with an increase in pH. Adhesion is believed to be promoted by reduced hydration of chitosan with increasing pH as polyelectrolyte hydration and osmotic potential of the polyelectrolyte hydrogel correlate with its charge density.⁵⁸ Dehydration of chitosan leads to increased density of physical bonds between chitosan segments as the disrupting hydration layer is diminished and electrostatic repulsion is reduced. Bonding between CNF and chitosan is also believed to increase with reducing hydration of chitosan. The interface between CNF and chitosan is suggested to be stronger than that between chitosan segments as ionic cross-linking of chitosan at low pH leads to a nearly 10-fold increase in tensile strength (see Figure 6b).

The exact mechanism of bonding between CNF and chitosan is complicated and remains unclear. The contributing interactions that have been suggested in the literature include hydrogen bonding, ionic interactions, covalent imine linkage, and hydrophobic interactions.^{37,46,59,60} Also, entropic contribu-

tion from release of organized water at the hydration layer is likely to contribute to bonding.²⁶ However, in the present work the contribution of ionic interactions to cross-linking may be neglected because after immersion to 100 mM NaOH the chitosan backbone is uncharged.⁴⁸ Contribution from covalent imine linkages between the aldehydes of the reducing ends of cellulose and primary amines of chitosan is considered possible.⁶¹ To single out the dominant contribution of permanent covalent imine linkages, we studied the reversibility of the effect of the base-treatment shown in Figure 5b. Therein, the drastic effect of base-treatment was largely reversed upon soaking a base-treated CNF/chitosan 80/20 w/w film in 100 mM HCl (aq) for 60 s prior to tensile measurement, instead of soaking in deionized water (Figure S5). This supports the claim that cross-linking occurs mostly by physical interactions promoted by dehydration of chitosan. Additionally, the effect of pH on mechanical properties is not explained by imine formation and the films produced were colorless. Extensive imine formation between cellulose and chitosan typically occurs at elevated temperatures and yields observable color in UV-vis spectra.⁶² Tentatively, multivalent hydrogen bonding and hydrophobic interactions between CNF and chitosan promoted by dehydration of chitosan with increasing pH are suggested to be the central cross-linking mechanisms.^{27–29,35,37,59,60}

Cyclic tensile characterization in the wet state was performed for CNF/chitosan 80/20 w/w samples to investigate whether the behavior is elastic or plastic, see Figure 8. The maximum

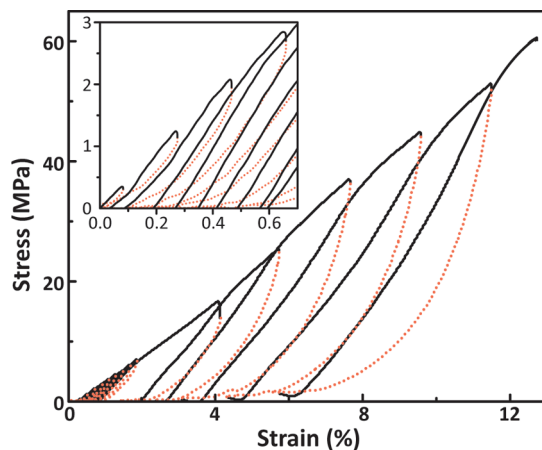


Figure 8. Cyclic tensile tests of the base-treated CNF/chitosan 80/20 w/w composition in the wet state. The inset shows short cycles at low stress and strain.

strain per cycle was increased with small steps at low strain, which is highlighted in the inset in Figure 8. Already in the first strain cycle the behavior seems to be highly plastic as the stress during the second strain cycle begins to rise at a strain only slightly lower than the maximum strain of the previous cycle. After the first cycle, the sample begins to demonstrate some elastic behavior also as the roughly half of the strain is recovered. This behavior continues also to larger deformations until fracture. The material clearly demonstrates strain-hardening also in the wet state as the stress needed to apply to cause further plastic deformation increases.⁶³ Young's moduli are calculated for each elongation step during cyclic loading for three samples (Figure S6).

Dense, covalent cross-linking of CNF could lead to highly brittle behavior of the material, but this is avoided with the

present physical cross-linking when using chitosan. This is highlighted by retaining the tensile stress-strain behavior of base-treated CNF/chitosan 80/20 w/w films of high strength also in a more dry state (relative humidity 50%, temperature 20 °C, film not wetted) very similar to that of the neat CNF films shown in Figure 9. In fact, the CNF/chitosan 80/20 w/w film is slightly softer and more extensible than the neat CNF film.

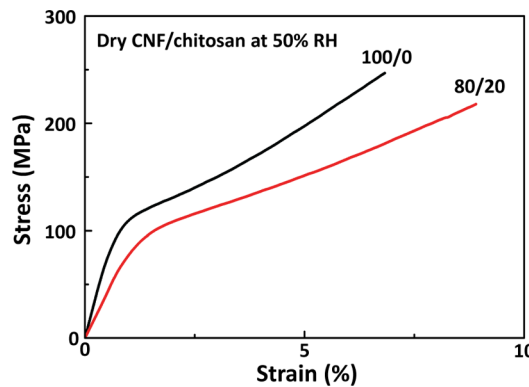


Figure 9. Stress-strain curve of dry base-treated CNF/chitosan 100/0 and 80/20 w/w at 50% relative humidity.

Optical Properties. Solvent casting of homogeneous mixtures results in highly transparent films, of which few millimeter-wide, base-treated strips are shown in Figure 10, alongside their UV-vis transmission spectra. No clearly visible differences in optical properties are observed between base-treated and not base-treated films. For most compositions, the films show high transparencies in the range of 400–800 nm,

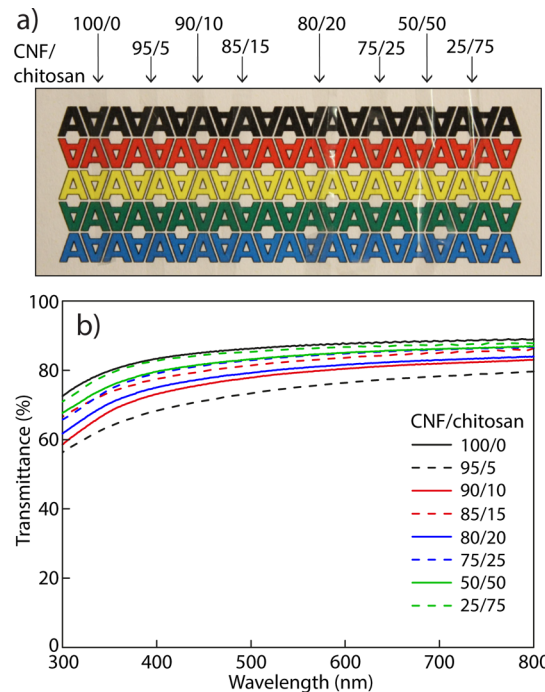


Figure 10. Photograph of cut strips (a) and UV-vis spectra (b) of base-treated thin films (10–13 μm) for different CNF/chitosan mixing ratios. Arrows indicate the positions of the films of different compositions, where the high transparency is illustrated by the fact that the films are barely resolved.

between approximately 70 and 90%. This is a significant improvement in comparison to previous CNF/chitosan reports, where transparency was reduced to below 70% at already 32% CNF and below 40% at 50% CNF.^{36,55} Visual inspection indicates that all films are approximately similar in transparency. UV-vis shows that the pure CNF film presented the highest transparency over the whole spectrum. The hybrid films have slightly lower transparencies. A trend is suggested, where the hybrid films have increasing transparency with increasing chitosan loading. This may result during mixing from slight aggregation of CNF by chitosan, which is enhanced when CNF-to-chitosan ratio is high.

The transparency of the CNF/chitosan hybrid nanopaper is a result of the subwavelength dimensions of the formed structures.^{4,5} Aggregates and poorly fibrillated material from the CNF dispersion can be separated from the more stable residual nanofibrillar component by centrifugation, as shown in Figure 3. The higher stability of the fibrils in the supernatant is due to their smaller dimensions compared to the solid matter in the sediment, but possibly also due to higher charge density resulting from elevated residual heteropolysaccharide content (mainly xylans), see Table S1. The difference in sizes of the structures is evident in the scanning electron micrographs of the surfaces of films evaporated from the supernatant and sediment, as shown in Figure 11. The insets therein show the difference in transparency between the sediment and supernatant even after adjustment to equal weight percent. In addition, the difference in transparency of the resulting films upon solvent casting is shown in the inset. The aggregates and unfibrillated material lead to voids and more dense areas that

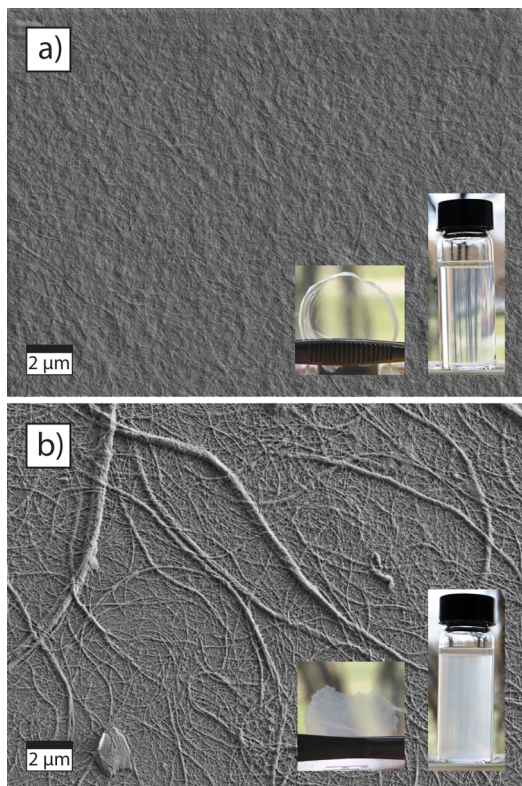


Figure 11. Scanning electron micrographs of films cast from (a) supernatant and (b) sediment of CNF after centrifugation for 1 h at 5000g. The insets show the corresponding dispersions both at 0.18 wt % and films cast from the dispersions.

are of the order of the wavelength of visible light or larger which leads to promoted light scattering. Homogenous mixtures and nanoscale dimensions of the components are shown in Figures S8–10, which show TEM micrographs of CNF/chitosan 80/20 w/w with chitosan stained for 10 min in methyl iodide vapor.

Orientation. Orientation can be induced in CNF films by drawing, as shown previously.^{64,65} Therein, special care is necessary in drawing of the neat CNF films in the wet state due to their low mechanical integrity. In our case, the drawing has been considerably easier since in the wet state the hybrid films were significantly stronger than the neat CNF films. Due to the transparency of the films, it was possible to follow the development of the orientation during the tensile testing using video *in-situ* between crossed polarizers. Figure 12 shows

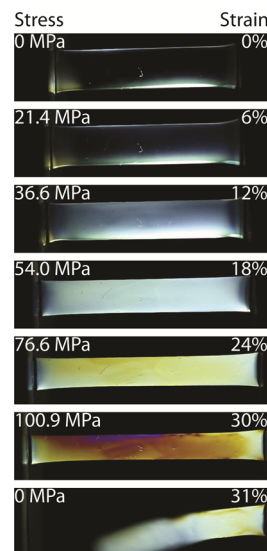


Figure 12. Optical images of wet CNF/chitosan 80/20 w/w under tension between crossed polarizers with illumination from below. Polarizer axes are at 45° with respect to the sample elongation direction.

video frames (original video in Supporting Information, see Movie S1) at different intervals showing the development of birefringence, which is proportional to Hermans orientation parameter $f = \Delta n / \Delta n_0$, where Δn is the birefringence of the material and Δn_0 is the maximum birefringence.⁵³ The colors seen between crossed polarizers change smoothly upon stretching (Figure 12). We interpret them using Michel-Lévy (Figure S11) and Raith-Sørensen birefringence charts (Figure S12).⁶⁶ For example, the birefringence of the 12.1 μm thick film depicted in Figure 12 reached a value of $\Delta n = 0.034\text{--}0.051$ in the violet edge at 30% elongation. The birefringence is reduced upon rupture of the film and subsequent relaxation, which can be seen also in the last frame of Figure 12. After rupture, Δn drops to roughly 0.015–0.030. These values could be compared with the commonly accepted value $\Delta n_0 = 0.074$ for a perfectly aligned crystal of native cellulose.⁶⁷ The above consideration would render the Hermans orientation parameter to lie between 0.459–0.689 before and 0.203–0.405 after rupture. This magnitude of drop in birefringence by roughly a factor of 2 corresponds well with the elastic behavior determined in cyclic tensile tests, where elastic strain is roughly half of the total strain per cycle.

Orientation of the base-treated CNF/chitosan 80/20 w/w films was further examined using WAXS experiments. Samples were stretched up to 0, 5, 10, 15, and 20% strains in the wet state and subsequently dried. Hermans orientation parameters were calculated from the intensity distribution profiles in the azimuthal angle along (200) reflection of the crystalline cellulose I β .⁵² Two exemplary diffractograms and their intensity distribution profiles in the azimuthal angle of samples with draw ratios 1.0 and 1.2 are shown in Figure 13a,b. The

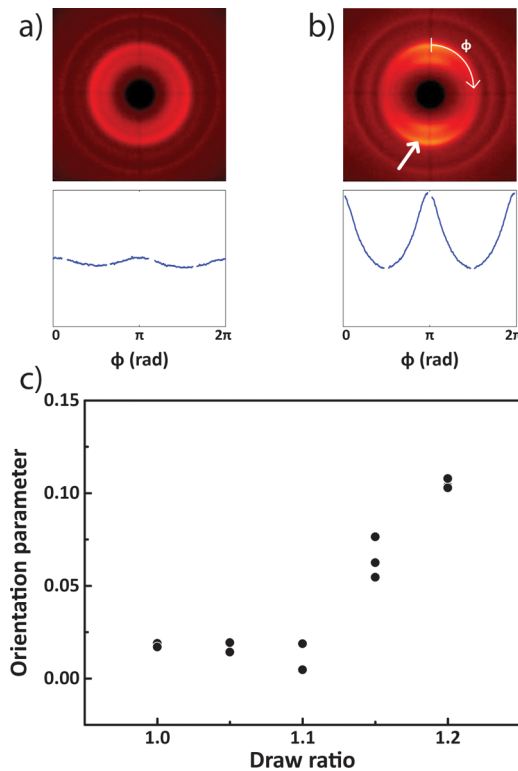


Figure 13. WAXS diffractograms of wet-stretched and dried base-treated CNF/chitosan 80/20 w/w films with draw ratios (a) 1.0 and (b) 1.2, corresponding to the intensity distribution profiles in the azimuthal angle (below diffractograms), and (c) orientation parameter vs draw ratio of films. The WAXS diffraction is highlighted with an arrow along which the intensity distribution profiles in the azimuthal angle are taken. Note that in the intensity distribution profiles the baselines are not adjusted to zero and both profiles are on the same scale enabling easier evaluation of the respective degree of orientation.

calculated orientation parameters of films versus their draw ratios are shown in Figure 13c. Measured orientation is negligible below draw ratio 1.1 and increases at higher draw ratios. The values are small compared to those reported in the literature since for comparable cold drawn CNF films a Hermans orientation factor of 0.36 was reported at a draw ratio of 1.2.⁶⁴ This is a 3-fold difference compared to the values obtained with the same draw ratio of 1.2 in this work. The reason for this difference is not clear, but it is possible that the chitosan chains cross-linking CNF fibrils are able to function as entropic springs retracting the structure back toward its original conformation when the sample is relaxed.

CONCLUSIONS

Hybrid nanopapers of CNF and chitosan were prepared and physically cross-linked to significantly improve their wet tensile properties by reducing hydration of chitosan inside the films

with a base-treatment. Already a small increase in chitosan content from 0 to 5% caused dramatic improvements in wet tensile properties when the film was base-treated with 100 mM NaOH solution. The base-treated CNF/chitosan 80/20 w/w film reached the highest wet tensile strength measured, 100 MPa. A maximum strain of at least 18% was recorded for all base-treated compositions with chitosan and many strained up to 25% without breaking. Tensile moduli increased with plastic strain from 4 and 14 GPa at low (0.5%) and large (16%) strains. Increasing the chitosan content to 75% increased the maximum strain further, but negatively affected tensile strength. A clear increase in wet strength was observed as the pH increased from 5.7 to 6.8, that is, from below to above the pK_a of chitosan. The wet strength of the base-treated CNF/chitosan was interpreted to result from cross-linking whereby chitosan tightly binds onto cellulose surfaces, probably via multivalent physical interactions. The physical cross-linking did not reduce the remarkable toughness of more dry hybrid nanopapers: a tensile strength of 200 MPa (with maximum strain of 8%) was measured at 50% air relative humidity for base-treated CNF/chitosan 80/20 w/w film. In addition, high transparency (~70–90% in the range of 400–800 nm) resulted from homogeneous mixtures, nanoscale dimensions of CNF fibrils and suppressed component aggregation leading to reduced diffraction of visible light. The presented new and simple approach of physical cross-linking expands the high mechanical properties of transparent CNF-based materials to the wet-state, as demanded in advanced applications.

ASSOCIATED CONTENT

Supporting Information

Material about additional data and images on the CNF used, CNF/chitosan mixtures, polarized optical video of a mechanical sample during tensile testing and films, and Michel-Lévy and Raith-Sørensen birefringence charts. This material is available free of charge via the Internet at <http://pubs.acs.org>.

AUTHOR INFORMATION

Corresponding Author

*E-mail: olli.ikkala@aalto.fi

Notes

The authors declare no competing financial interest.

ACKNOWLEDGMENTS

This work was carried out under the Academy of Finland Centres of Excellence Programme (2014–2019) and supported by the Academy of Finland Project 264677. The authors also thank Dr. Andreas Walther for instructions (CellAssembly project in ERA-Net). F.H.S. is grateful to the Thuringian Ministry for Science, Education and Culture (TMBWK) for financial support (Grant #BS15-11028). Aalto Nanomicroscopy Center is acknowledged for the use of the devices.

REFERENCES

- Moon, R. J.; Martini, A.; Laird, J.; Simonsen, J.; Youngblood, J. *Chem. Soc. Rev.* 2011, 40, 3941–3994.
- Saito, T.; Kuramae, R.; Wohlert, J.; Berglund, L. A.; Isogai, A. *Biomacromolecules* 2013, 14, 248–253.
- Henriksson, M.; Berglund, L. A.; Isaksson, P.; Lindström, T.; Nishino, T. *Biomacromolecules* 2008, 9, 1579–1585.
- Nogi, M.; Iwamoto, S.; Nakagaito, A. N.; Yano, H. *Adv. Mater.* 2009, 21, 1595–1598.

- (5) Yano, H.; Sugiyama, J.; Nakagaito, A. N.; Nogi, M.; Matsuura, T.; Hikita, M.; Handa, K. *Adv. Mater.* **2005**, *17*, 153–155.
- (6) Siqueira, G.; Bras, J.; Dufresne, A. *Polymers* **2010**, *2*, 728–765.
- (7) Rhim, J.-W.; Park, H.-M.; Ha, C.-S. *Prog. Polym. Sci.* **2013**, *38*, 1629–1652.
- (8) Koga, H.; Nogi, M.; Komoda, N.; Nge, T. T.; Sugahara, T.; Suganuma, K. *NPG Asia Mater.* **2014**, *6*, e93.
- (9) Huang, J.; Zhu, H.; Chen, Y.; Preston, C.; Rohrbach, K.; Cumings, J.; Hu, L. *ACS Nano* **2013**, *7*, 2106–2113.
- (10) Nagashima, K.; Koga, H.; Celano, U.; Zhuge, F.; Kanai, M.; Rahong, S.; Meng, G.; He, Y.; Boeck, J. D.; Jurczak, M.; Vandervorst, W.; Kitaoka, T.; Nogi, M.; Yanagida, T. *Sci. Rep.* **2014**, *4*, 5532.
- (11) Fang, Z.; Zhu, H.; Yuan, Y.; Ha, D.; Zhu, S.; Preston, C.; Chen, Q.; Li, Y.; Han, X.; Lee, S.; Chen, G.; Li, T.; Munday, J.; Huang, J.; Hu, L. *Nano Lett.* **2014**, *14*, 765–773.
- (12) Benítez, A. J.; Torres-Rendon, J.; Poutanen, M.; Walther, A. *Biomacromolecules* **2013**, *14*, 4497–4506.
- (13) Malho, J.-M.; Ouellet-Plamondon, C.; Rüggeberg, M.; Laaksonen, P.; Ikkala, O.; Burgert, I.; Linder, M. B. *Biomacromolecules* **2014**, *16*, 311–318.
- (14) Back, E. L.; Klinga, L. O. *Tappi J.* **1963**, *46*, 284–288.
- (15) Caulfield, D. F. *Tappi J.* **1994**, *77*, 205–212.
- (16) Spoljaric, S.; Salminen, A.; Luong, N. D.; Seppälä, J. *Cellulose* **2013**, *20*, 2991–3005.
- (17) Nakagaito, A. N.; Yano, H. *Appl. Phys. A: Mater. Sci. Process* **2005**, *80*, 155–159.
- (18) Henriksson, M.; Berglund, L. A. *J. Appl. Polym. Sci.* **2007**, *106*, 2817–2824.
- (19) Ansari, F.; Galland, S.; Johansson, M.; Plummer, C. J. G.; Berglund, L. A. *Composites, Part A* **2014**, *63*, 35–44.
- (20) Omidian, H.; Park, K. Introduction to Hydrogels. In *Biomedical Applications of Hydrogels Handbook*; Ottenbrite, R. M., Park, K., Okano, T., Eds.; Springer: New York, 2010; p 11.
- (21) Bagheri, R.; Marouf, B. T.; Pearson, R. A. *J. Macromol. Sci., Polym. Rev.* **2009**, *49*, 201–225.
- (22) Sun, J.-Y.; Zhao, X.; Illeperuma, W. R. K.; Chaudhuri, O.; Oh, K. H.; Mooney, D. J.; Vlassak, J. J.; Suo, Z. *Nature* **2012**, *489*, 133–136.
- (23) Henderson, K. J.; Zhou, T. C.; Otim, K. J.; Shull, K. R. *Macromolecules* **2010**, *43*, 6193–6201.
- (24) Zhao, X. *Soft Matter* **2014**, *10*, 672–687.
- (25) Fantner, G. E.; Oroodjev, E.; Schitter, G.; Golde, L. S.; Thurner, P.; Finch, M. M.; Turner, P.; Gutmann, T.; Morse, D. E.; Hansma, H.; Hansma, P. K. *Biophys. J.* **2006**, *90*, 1411–1418.
- (26) Mammen, M.; Choi, S.-K.; Whitesides, G. M. *Angew. Chem., Int. Ed.* **1998**, *37*, 2754–2794.
- (27) Jean, B.; Heux, L.; Dubreuil, F.; Chambat, G.; Cousin, F. *Langmuir* **2009**, *25*, 3920–3923.
- (28) Yokota, S.; Ohta, T.; Kitaoka, T.; Ona, T.; Wariishi, H. *Sen’i Gakkaishi* **2009**, *8*, 212–217.
- (29) Majoinen, J.; Haataja, J. S.; Appelhans, D.; Lederer, A.; Olszewski, A.; Seitsonen, J.; Aseyev, V.; Kontturi, E.; Rosilo, H.; Österberg, M.; Houbenov, N.; Ikkala, O. *J. Am. Chem. Soc.* **2014**, *136*, 866–869.
- (30) McKee, J. R.; Hietala, S.; Seitsonen, J.; Laine, J.; Kontturi, E.; Ikkala, O. *ACS Macro Lett.* **2014**, *3*, 266–270.
- (31) Walther, A.; Timonen, J. V. I.; Díez, I.; Laukkanen, A.; Ikkala, O. *Adv. Mater.* **2011**, *23*, 2924–2928.
- (32) Iwamoto, S.; Isogai, A.; Iwata, T. *Biomacromolecules* **2011**, *12*, 831–836.
- (33) Håkansson, K. M. O.; Fall, A. B.; Lundell, F.; Yu, S.; Krywka, C.; Roth, S. V.; Santoro, G.; Kvick, M.; Wittberg, L. P.; Wågberg, L.; Söderberg, L. D. *Nat. Commun.* **2014**, *5*, 4018.
- (34) Vollrath, F.; Knight, D. P. *Nature* **2001**, *410*, 541–548.
- (35) Nordqvist, D.; Idermark, J.; Hedenqvist, M. S. *Biomacromolecules* **2007**, *8*, 2398–2403.
- (36) Wu, T.; Farnood, R.; O’Kelly, K.; Chen, B. *J. Mech. Behav. Biomed. Mater.* **2014**, *32*, 279–286.
- (37) Myllytie, P.; Salmi, J.; Laine, J. *BioResources* **2009**, *4*, 1647–1662.
- (38) Orelma, H.; Filpponen, I.; Johansson, L.-S.; Laine, J.; Rojas, O. J. *Biomacromolecules* **2011**, *12*, 4311–4318.
- (39) Arboleda, J. C.; Niemi, N.; Kumpunen, J.; Lucia, L. A.; Rojas, O. J. *ACS Sustainable Chem. Eng.* **2014**, *2*, 2267–2274.
- (40) Rinaudo, M. *Prog. Polym. Sci.* **2006**, *31*, 603–632.
- (41) Kong, M.; Chen, X. G.; Xing, K.; Park, H. J. *Int. J. Food Microbiol.* **2010**, *144*, 51–63.
- (42) Shahidi, F.; Arachchi, J. K. V.; Jeon, Y.-J. *Trends Food Sci. Technol.* **1999**, *10*, 37–51.
- (43) Ravi Kumar, M. N. V.; Muzzarelli, R. A. A.; Muzzarelli, C.; Sashiwa, H.; Domb, A. J. *Chem. Rev.* **2004**, *104*, 6017–6084.
- (44) Lindström, T.; Wågberg, L.; Larsson, T. On the nature of joint strength in paper – a review of dry and wet strength resins used in paper manufacturing. In *Advances in Paper Science and Technology*; I’Anson, S. J., Ed.; Trans. XIIth Fund. Res. Symp. Cambridge; FRC: Manchester, 2005; pp 501–503.
- (45) Laleg, M.; Pikulik, I. I. *Nord. Pulp Pap. Res. J.* **1991**, *6*, 99–103.
- (46) Laleg, M.; Pikulik, I. *Nord. Pulp Pap. Res. J.* **1992**, *7*, 174–180.
- (47) Li, H.; Du, Y.; Xu, Y. *J. Appl. Polym. Sci.* **2004**, *91*, 2642–2648.
- (48) Rinaudo, M.; Pavlov, G.; Desbrières, J. *Polymer* **1999**, *40*, 7029–7032.
- (49) Park, J. W.; Choi, K.-H.; Park, K. K. *Bull. Korean Chem. Soc.* **1983**, *4*, 68–72.
- (50) Sluiter, A.; Hames, B.; Ruiz, R.; Scarlata, C.; Sluiter, J.; Templeton, D.; Crocker, D. *NREL/TP-510-42618*; National Renewable Energy Laboratory: Golden, CO, 2008.
- (51) Czechowska-Biskup, R.; Jarosińska, D.; Rokita, B.; Ulański, P.; Rosiak, J. M. *Prog. Chem. Appl. Chitin Its Deriv.* **2012**, *17*, 5–20.
- (52) Sugiyama, J.; Vuong, R.; Chanzy, H. *Macromolecules* **1991**, *24*, 4168–4175.
- (53) Gedde, U. W. *Polymer Physics*; Chapman & Hall: Suffolk, U.K., 1996; p 203.
- (54) Pääkkö, M.; Ankerfors, M.; Kosonen, H.; Nykänen, A.; Ahola, S.; Österberg, M.; Ruokolainen, J.; Laine, J.; Larsson, P. T.; Ikkala, O.; Lindström, T. *Biomacromolecules* **2007**, *8*, 1934–1941.
- (55) Fernandes, S. C. M.; Freire, C. S. R.; Silvestre, A. J. D.; Pascoal Neto, C.; Gandini, A.; Berglund, L. A.; Salmén, L. *Carbohydr. Polym.* **2010**, *81*, 394–401.
- (56) Brady, J. W.; Schmidt, R. K. *J. Phys. Chem.* **1993**, *97*, 958–966.
- (57) Fringant, C.; Tvaroska, I.; Mazeau, K.; Rinaudo, M.; Desbrieres, J. *Carbohydr. Res.* **1995**, *278*, 27–41.
- (58) Omidian, H.; Park, K. Introduction to Hydrogels. In *Biomedical Applications of Hydrogels Handbook*; Ottenbrite, R. M., Park, K., Okano, T., Eds.; Springer: New York, 2010; p 4.
- (59) Nordgren, N.; Eronen, P.; Österberg, M.; Laine, J.; Rutland, M. W. *Biomacromolecules* **2009**, *10*, 645–650.
- (60) Lindman, B.; Karlström, G.; Stigsson, L. *J. Mol. Liq.* **2010**, *156*, 76–81.
- (61) Hosokawa, J.; Nishiyama, M.; Yoshihara, K.; Kubo, T.; Terabe, A. *Ind. Eng. Chem. Res.* **1991**, *30*, 788–792.
- (62) Urreaga, J. M.; de la Orden, M. U. *Eur. Polym. J.* **2006**, *42*, 2606–2616.
- (63) Crandall, S. H.; Dahl, N. C.; Lardner, T. J. Stress-Strain-Temperature Relations. In *An Introduction to the Mechanics of Solids*; Lardner, T. J., Ed.; McGraw-Hill: New York, 1978; pp 276–277.
- (64) Sehaqui, H.; Mushi, N. E.; Morimune, S.; Salajkova, M.; Nishino, T.; Berglund, L. A. *ACS Appl. Mater. Interfaces* **2012**, *4*, 1043–1049.
- (65) Torres-Rendon, J. G.; Schacher, F. H.; Ifuku, S.; Walther, A. *Biomacromolecules* **2014**, *15*, 2709–2717.
- (66) Sørensen, B. E. *Eur. J. Mineral.* **2013**, *25*, 5–10.
- (67) Bordel, D.; Putaux, J.-L.; Heux, L. *Langmuir* **2006**, *22*, 4899–4901.